

1 **MONITORING SECONDARY STRUCTURAL CHANGES IN SALTED AND SMOKED**
2 **SALMON MUSCLE MYOFIBER PROTEINS BY FT-IR MICROSPECTROSCOPY.**

3 Izaskun Carton^{1,2*}, Ulrike Böcker¹, Ragni Ofstad¹, Oddvin Sørheim¹ and Achim Kohler^{1,3,4}

4

5 ¹Matforsk AS, Nofima Food, and Centre for Biospectroscopy and Data Modelling,
6 Osloveien 1, N-1430 Ås, Norway

7 ²Food Technology, Faculty of Pharmacy, University of the Basque Country (EHU-UPV),
8 Paseo de la Universidad No. 7, 01006 Vitoria-Gasteiz, Spain

9 ³CIGENE, Centre for Integrative Genetics, Norwegian University of Life Sciences, N-1432
10 Ås, Norway

11 ⁴Department of Mathematical Sciences and Technology (IMT), Norwegian University of Life
12 Sciences, N-1432 Ås, Norway

13

14 **Running title: FTIR spectroscopy of smoked salmon myofibrillar proteins**

15

16 ***corresponding author:**

17 Izaskun Carton

18 Food Technology, Faculty of Pharmacy, University of the Basque Country (EHU-UPV),

19 Paseo de la Universidad No. 7, 01006

20 Vitoria-Gasteiz, Spain

21 Phone: +34 943 01 30 84

22 e-mail: izaskun.carton@ehu.es

23

24

25

1 **ABSTRACT**

2 Fourier transform infrared (FTIR) microspectroscopy and light microscopy were used to
3 study changes in the myofibrillar proteins and microstructure in salmon muscle due to dry
4 salting and smoking. Light microscopy showed that the myofibers of the smoked samples
5 were more shrunken and their shape more irregular and edged than for the non-smoked
6 samples. FTIR microspectroscopy showed that salting time mostly contributed in the amide I
7 region, revealing that secondary structural changes of proteins were primarily affected by
8 salting. The main variation in amide II region was caused by smoking. As it is known that
9 smoke components can react with amino acid side chains and that the contribution of the side
10 chain in the amide II region is larger than in the amide I, it is concluded that the observed
11 differences are due to interactions between carbonyl compounds of smoke and amino acid
12 side chains .

13

14

15

16

17

18

19

20

21

22 Keywords: FT-IR microspectroscopy, myofibrillar proteins, salmon, salting, smoking

23

24

25

1 INTRODUCTION

2 Traditionally, cold smoked salmon is a highly valued product. Cold smoking is a process by
3 which the fish is submitted to salting before being smoked at temperatures around 25°C
4 without further heat treatment. It is categorized as “lightly preserved” product and thus there
5 is a need for improved knowledge about which processing parameters influence product
6 quality.

7 Salting is the first step in the smoking process and is crucial to obtain high shelf-life, good
8 quality and yield of the product. The salt may be added through dry salting, brine salting, or
9 injection. Dry salting is the most common technique for processing cold smoked salmon (1).
10 Salting time varies between smoke houses from hours to several days (2). Salting is known to
11 influence texture properties and water holding capacity (3). Barat and co-workers (4)
12 suggested that during salting some of the proteins are denatured and precipitate as a result of
13 the high ionic forces in the media, giving rise to textural changes in the product. A recent
14 study by Böcker and co-workers (5) investigated the effects of brine salting (16% NaCl) on
15 protein structure in Atlantic salmon muscle tissue with respect to raw material variation. The
16 highest salt uptake was achieved for frozen/thawed (4.1%), followed by post-rigor (3.0%) and
17 pre-rigor (2.2%) salmon, respectively. They observed that samples with a lower salt uptake
18 experienced less swelling of the myofibers.

19 It is known that the smoking process increases the shelf-life of fish as a result of the combined
20 effects of dehydration, antimicrobial (6), and antioxidant activity (7) of several of the smoke
21 components such as formaldehyde, carboxylic acids and phenols (8-9). Few studies have
22 addressed the effect of the smoking process in salmon myofibrillar proteins. Most of the
23 authors suggested that salt is the most important factor for textural and microstructural
24 changes. Sigurgisladottir and co-workers (10) demonstrated that salmon muscle fibers shrink
25 during the smoking process. It was also shown that the amount of salt-soluble proteins in

1 salmon is reduced by smoking (11-12). Previous studies report that interactions between
2 smoke components and amino groups of proteins exist, especially formaldehyde as a smoke
3 component, with the ε-amino group of lysine (13-17).
4 Although it is known that the smoking process evokes reactions with amino-acid side chains,
5 the influence of the smoking process on protein secondary structure and textural properties is
6 still a rather unexplored field. Fourier Transform Infrared (FT-IR) spectroscopy has been
7 widely used to study protein secondary structure (18) and in recent years it has become an
8 increasingly powerful tool for the analysis of protein secondary structure in intact food tissues
9 (5, 19-24). The main advantage of FT-IR microspectroscopy is that it can be easily combined
10 with histological investigations, as it requires a similar sample preparation, and thus, specific
11 features can be studied on parallel sections both spectroscopically and histochemically.
12 Kirschner and co-workers (19) used FTIR-microspectroscopy to monitor heat-induced
13 denaturation in beef muscle. Recently, this technique has been used to characterize
14 processing-induced changes (salting and heating among others) on myofibrillar protein
15 structure of pork muscle and salmon fillets (5, 20-24).
16 The objective of this paper was to investigate structural changes in salmon muscle during
17 salting and smoking by FT-IR microspectroscopy and light microscopy. While the effect of
18 salting on protein structure has been previously studied by FT-IR microspectroscopy, we
19 intended to investigate if this technique can detect changes of protein secondary structure as a
20 function of smoking.

21

22

23 **MATERIALS AND METHODS**

24 **Sample preparation.** 9 farmed salmon (*Salmo salar*) of different size (small, 3-4 kg; medium,
25 4-5 kg; and large, 5-6 kg) were acquired from a commercial fish company (Bremnes Seashore

1 AS, Bremnes, Norway). After gutting and cleaning, they were manually filleted pre-rigor on the
2 day of harvest. To study the influence of the salting time, 6 of the 9 salmons were dry salted at
3 4 °C, their left fillets for 24 hours, and right fillets for 8 hours. After the salting and an
4 equilibration period of 4 days at 4°C, half of the samples were smoked: 3 fillets from each type
5 of salting were smoked in a smoking chamber (Unimatic Smoking Unit equipped with a
6 Unitronic SC 2000 Control Unit, Doleschal, Austria) with smoke generated from beech wood for
7 5.5 hours at 28 °C. Finally, 3 of the 9 salmons were used for collecting unprocessed samples.
8 Moreover, all individual fillets were weighed out before and after each process to know the
9 weight loss caused by salting or smoking.

10 This resulted in a total of 5 different groups; (1) unprocessed samples (n=3), (2) samples salted
11 for 8 hours (n=3), (3) samples salted for 24 hours (n=3), (4) samples salted for 8 hours followed
12 by smoking (n=3) and (5) samples salted for 24 hours followed by smoking (n=3). Sampling for
13 chemical analyses (salt and fat determination) was done for each condition at head and tail
14 regions. Additionally, for light microscopy and FTIR microspectroscopy, samples from skinside
15 (approximately 2 mm from the skin) and inside locations (approximately 30 mm from the skin)
16 were also taken at head and tail regions for each individual, respectively. Blocks of about 0.7 cm
17 x 0.7 cm x 0.2 cm were excised and embedded in O.C.T. compound (Tissue-Tek, Electron
18 Microscopy Sciences, Hatfield, PA) and then snap-frozen in liquid N₂. The samples were stored
19 at -80°C until cryo-sectioning for light microscopy and FT-IR measurements. 10 µm thick
20 cryosections were cut on a Leica CM3050S Cryostat (Leica, Nussloch, Germany).

21 **Chemical Analysis.** NaCl content in the samples was determined as water soluble Cl⁻ by
22 titration with a Corning Salt Analysator 926 (Chloride analyzer 926 Corning, Corning
23 Medical and Scientific, Halstead, England) (25). The fat content was measured using a low-
24 field ¹H-NMR instrument (Maran Ultra, 23 MHz, Oxford 5 Instruments, UK). The instrument
25 was calibrated with refined salmon oil prior to analysis. Except for temperature

1 standardization, no further sample preparation was performed. The weight of the fillets was
2 registered before (w1) and after (w2) each process to calculate the weight loss according to
3 the following equation (1):

$$4 \quad \text{Weight loss \%} = (w1-w2)/w1 \times 100 \quad [1]$$

5 The results given in table 1 for salt and fat content are based on duplicated determinations and
6 are presented as average values together with their standard deviations. In addition, the
7 significance of the differences was determined by use of *t* test.

8 **Light Microscopy.** For light microscopy, cryosections were stained with 1g/100ml Toluidine
9 Blue (Sigma-Aldrich Norway AS, Oslo, Norway) to elucidate the general structure of the
10 muscle samples. The sections were examined with a Leica DM 6000B microscope (Leica
11 Microsystems Wetzlar GmbH, Wetzlar, Germany) and images were acquired at 10 x
12 magnification with an Evolution MP 5.0 CCD Camera (Media Cybernetics, The Imaging
13 Experts Silver Springs, Maryland, USA). The images taken as light micrographs correspond
14 to the same areas from which spectra were collected by FT-IR microspectroscopy on parallel
15 cryo-sections.

16 **FT-IR microspectroscopy and pre-processing of the FT-IR spectra.**

17 For FT-IR microspectroscopy, the cryosections were thaw-mounted on 3 mm thick ZnSe
18 slides and were stored overnight in a desiccator at room temperature before the
19 measurements. The FT-IR measurements were carried out with an IRscope II combined with
20 an Equinox 55 FT-IR spectrometer (both Bruker Optics, Germany). Spectra were collected
21 from single myofibers in transmission mode in the frequency range from 4000 to 1000 cm⁻¹
22 using a mercury cadmium telluride (MCT) detector. For each spectrum, 256 interferograms
23 were co-added and averaged at a resolution of 6 cm⁻¹. The microscope and the spectrometer
24 were purged with dry air to reduce spectral contributions from water vapor and CO₂. A

1 background spectrum of the ZnSe substrate was recorded before each spectrum was measured
2 in order to account for variations in water vapor and CO₂.

3 For every sample two different blocks were analyzed. From every block one cryosection was
4 prepared and three spectra were acquired from three different myofibers per section resulting
5 in total in 180 spectra: 3 spectra from each cryosection x 4 locations (skinside and inside at
6 head and tail regions, respectively) x 5 conditions (unprocessed, salted for 8 h, salted for 24 h,
7 salted for 8 h with subsequent smoking and salted for 24 h with subsequent smoking) x 3
8 biological replicates (individual fishes) per condition. Spectra were pre-processed by taking
9 second derivatives applied a nine point Savitzky-Golay filter (26), followed by extended
10 multiplicative signal correction in the spectral range 3200-1000 cm⁻¹ (27).

11 **Data Analysis.** The 180 FT-IR spectra from each block were averaged resulting in just one
12 spectrum per experimental condition, in total 60 mean spectra. The data analysis was carried
13 out using Principal Component Analysis (PCA) and Partial Least Squares Regression (PLSR).
14 PCA was used for the extraction and interpretation of systematic variance in multidimensional
15 data sets by means of a small number of non-correlated variables. PCA finds directions in the
16 data that explain most of the variation (28). These new orthogonal directions are linear
17 combinations of the original ones and are ordered with respect to the amount of explained
18 variance. In this paper, PCA was used to investigate the variation in amide I and II regions as
19 a function of salting and smoking processes Multivariate analysis was done both on mean-
20 spectra and on non-averaged spectra, resulting in the same variation patterns.

21 In PLSR only that part of the main variation in a data matrix **X** is extracted that at the same
22 time maximizes the variation in a data matrix **Y**, i.e. PLSR aims at using only the most
23 relevant part of the variation in **X** for the regression of **Y**, while the unstable or irrelevant
24 variation in **X** is left out of the calculation. In this study, the design variables were used as the
25 **X**-matrix and the measured variables (FT-IR data) were used as **Y**-matrix (28). The results of

1 PLSR were then studied using so-called correlation loading plots. The correlation loading plot
2 shows the correlation of the **X** and **Y** variables to the PLSR components (scores). Since in
3 second-derivative spectra minima are referring to spectral bands, the spectra were multiplied
4 by -1 before analysis by PLSR in order to facilitate interpretation.

5 All preprocessing and data analysis was performed using an in-house program written in
6 Matlab version 7.3 (The MathWorks, Natick, MA) and using The Unscrambler[®] version 9.2
7 (Camo Process AS, Norway).

8

9 **RESULTS AND DISCUSSION**

10 **Chemical Analysis and microstructure.**

11 **Table 1** shows the results obtained for weight loss, salt and fat content in processed samples,
12 expressed as percentage values, together with their standard deviation and the significance
13 level between samples. As expected, salt contents are significantly higher in samples salted
14 for 24 hours compared to the samples salted for 8 hours. Moreover, the highest salt contents
15 are found in the tail samples. A significant effect of salt concentration on weight loss ($P <$
16 $0,05$) is observed, being in average $6,45\% \pm 0,26$ and $4,86\% \pm 0,64$ for samples salted for 24
17 hours and 8 hours respectively. As it could also be observed in **Table 1**, the fat distribution on
18 studied fillets is not homogeneous, as it has been demonstrated by other authors (5, 29),
19 decreasing from the head region ($17,1\% \pm 1,9$) towards the tail ($6,0\% \pm 1,3$). In addition, the
20 flesh near the tail is thinner than in the head region. Therefore the salt penetrates more deeply
21 in the tail part. Several authors have reported that salt uptake in muscle is reduced by
22 increasing fat content (30-31).

23 Moreover, smoking shows significant effects on weight loss ($P < 0,001$), which can be
24 ascribed to the dehydration of the flesh after the smoking process. Therefore salt
25 concentrations are higher in smoked samples than in non-smoked ones. In addition, salt

1 content and weight loss values for smoked fillets show that samples salted for 24 hours
2 contained generally more salt than the samples salted only for 8 hours. The weight loss of the
3 fillets decreases from $9,18\% \pm 0,51$ to $8,03\% \pm 0,99$ as a function of salting time.

4 **Figure 1** shows selected images of transverse cryosections of samples from head region. As it
5 can be observed, unprocessed samples exhibit a structure with the myofibers appearing well-
6 attached. For the unprocessed sample there is no microstructural difference between the
7 skinside and the inside. After salting, clear differences between the inside and the skinside can
8 be seen. The inside samples are more detached and the extracellular spaces increase with the
9 salting time. This is due to the fact that during dry salting, the salt ions diffuse through the
10 muscle tissue by osmotic forces between the surrounding brine and the muscle, showing
11 shrinkage of the muscle fibers. The differences between skinside and inside samples can be
12 explained by the fact that the lipid content in the skinside is higher leading to a decrease of the
13 salt diffusivity (32).

14 After the smoking process, the differences appear to be even bigger: After salting for 24
15 hours, the myofibers of the smoked samples appear to be more shrunken and their shape
16 appears more irregular and edged than for the non-smoked samples. This is in agreement with
17 the results obtained by Sigurgisladdottir and co-workers (10). After salting for 8 hours, the
18 effect of smoking was not so strong. Also the skinside part of smoked samples was subjected
19 to only minor changes.

20 **FT-IR Microspectroscopy.**

21 **Figure 2** displays a typical spectrum of a single myofiber obtained from a fresh salmon
22 muscle cryosection in the spectral region from 4000 to 1000 cm^{-1} . This spectrum represents
23 the most typical features observed for the 5 groups investigated. The amide I ($1700\text{-}1600 \text{ cm}^{-1}$)
24 is the most dominant band in the myofiber spectrum. Of all the amide bands, of which there
25 exist nine, the amide I was found to be the most useful for the analysis of secondary structure

1 of proteins because of its sensitivity to hydrogen-bonding pattern, dipole-dipole interaction,
2 and the geometry of the polypeptide backbone (18, 33). It is mainly affected by the C=O
3 stretching vibration with a minor contribution of C-N stretching and N-H bending vibrations.
4 To enhance spectral resolution and gain insight in changes related to secondary structure of
5 the myofibrillar proteins, the amide I regions was investigated as second derivative spectra. In
6 the upper left corner of **Figure 2** the corresponding second derivative spectrum in the amide I
7 region for two exemplary spectra of unprocessed and processed samples are shown. In the
8 second derivative spectra of the amide I region we were able to identify and assign 9 bands
9 (1694, 1682, 1667, 1658, 1653, 1639, 1628, 1619 and 1609 cm^{-1}). Our findings are in
10 agreement with earlier studies on fish, pork and beef tissues (5, 19-24). The band assignments
11 are listed in **Table 2**.

12 *Spectral differences within unprocessed samples.*

13 Principal Component Analysis (PCA) was performed to study the unprocessed samples in the
14 amide I region (1700-1600 cm^{-1}). The score plot of the first and second principal component
15 based on 36 myofiber spectra (inside/skinside, head/tail, 3 different sizes) did not reveal any
16 systematic clustering of the samples according to individual or sample position (results not
17 shown). Higher principal components were also examined and no systematic variations could
18 be found. From these results, it can be concluded that, for the unprocessed samples, myofiber
19 FTIR spectra from different individuals and different locations show no systematic variation
20 with respect to local variation within each salmon fillet and individuals.

21 *Multivariate Analysis of myofiber spectra from processed salmon, non-smoked and smoked* 22 *samples.*

23 *Analysis of amide I*

24 PCA was used to investigate non-averaged spectra of (salted) non-smoked and smoked
25 samples in the amide I region (1700-1600 cm^{-1}) (shown in **Figure 3**). The explained variance

1 for PC1 and PC2 are 46% and 34% respectively. The first principal component showed a
2 systematic variation with respect to depth (difference between inside and skinside), whereas
3 the second principal component showed a systematic variation with respect to smoking.
4 Inspecting the loading vector of component one, we found that the band near 1653 cm^{-1} ,
5 which is α -helical structures, contributed strongly (results not shown). It was shown that this
6 band decreased in magnitude in inside samples of salmon fillets if we compare with skinside
7 samples, implying a loss of α -helical components. This may be explained by the fact that the
8 skin of the fish protects the flesh near the skin from salt and smoke components. In addition,
9 the fat deposited in the fish muscle acts as a barrier against the diffusion of these components
10 from the inside to muscle regions near the skin during processing; consequently the skin side
11 locations are less accessible. In the following we treat spectra from inside and skinside
12 locations separately.

13 PLSR was carried out to study the effect of the design factors on the FTIR spectra of
14 processed samples for skinside and inside samples separately. In the analysis, the X matrix
15 contained the design parameters while the Y matrix consisted of selected wavenumbers in the
16 amide I region. In **Figures 4a** and **4b** the correlation loading plots of the first two PLS
17 components of inside and skinside respectively are shown. The inner and outer circles in the
18 figures refer to 50 and 100% explained variance, respectively. For the inside part samples (**4a**)
19 the explained variance in X and Y for PLS component 1 and 2 are 23%, 23% for X and 36%
20 and 21% for Y . As **Figure 4a** shows, the salting time spans out the first PLS component while
21 smoking spans the second PLS component. Samples salted for 24 hours were highly
22 correlated with the bands 1628 , 1694 , 1682 and 1667 cm^{-1} , whereas samples salted for 8 hours
23 were well correlated with the band near 1653 cm^{-1} . This shows that longer salting periods
24 resulting in higher salt concentrations (see **Table 1**) lead to a higher share of β -sheet
25 structures and nonhydrogenated $\text{C}=\text{O}$ groups and a lower share of α -helical structure in the

1 myofibers (see **Table 2**). These findings support the result obtained by previous studies
2 related to different salt concentrations (20, 34). Böcker and co-workers (20) showed that in
3 pork muscle tissue subjected to brine salting at different salt concentration (0.9, 3, 6, and 9%
4 NaCl) the amount of α -helical structures (1653 cm^{-1}) was higher in samples with low salt
5 content and the level of nonhydrogenated C=O groups (1668 cm^{-1}) was increased at higher
6 salt concentrations. In another study (22) also in pork tissue subjected to salting at different
7 concentration (3, 6, and 9% NaCl) revealed that salting induced an increase in aggregated β -
8 sheet structure and a decrease in α -helical structure. A recent study by Böcker and co-workers
9 (5) on brine salting (16% NaCl) of Atlantic salmon showed that the salt uptake varied due to
10 the salmon raw material quality. The qualities which had higher salt content in the muscle
11 presented an increase in the share of the 1668 cm^{-1} band.

12 Smoked and non-smoked samples were separated along PLS 2. For non-smoked samples the
13 absorbances at the bands near 1639 cm^{-1} and 1609 cm^{-1} were increased. The band at 1639 cm^{-1}
14 was assigned both to antiparallel β -sheet structures (intramolecular) (18) and to O-H
15 bending of water (35). Since smoked samples show a higher weight loss than non-smoked
16 ones (see table 1), the decrease of absorption at 1639 cm^{-1} for smoked sample may be
17 explained by dehydration. Dehydration after smoking has been reported by several authors
18 (11-12). The band at 1609 cm^{-1} has frequently been discussed to be related to amino acid side
19 chains (36). In previous studies on muscle fiber tissues, this band has been tentatively
20 assigned to the amino acid tyrosine (23-24). Since carbonyl compounds of smoke can react
21 with amino groups of protein chain and/or of the side chains as in a Maillard reaction, we may
22 expect that in the present study the band at 1609 cm^{-1} is decreased in smoked samples, which
23 is confirmed by Fig. 4a.

24 For the skinside part samples (4b) the explained variance in **X** and **Y** for PLS component 1
25 and 2 was 22% and 22% for **X** and 32% and 14% for **Y**, respectively. In contrast to the inside

1 samples, for the skinside samples, PLS1 is mainly explained by the smoking and to a lower
2 degree by the salting time. This means that smoking introduces larger variations in the amide
3 I region than salting time. Apart from this, the general picture in Fig. 4b is unchanged and
4 confirms the findings from Fig. 4a.

5 *Analysis of amide II*

6 In the second derivative spectra of the amide II region (1600-1500 cm^{-1}), the following bands
7 were identified: 1584, 1574, 1567, 1555, 1544, 1534, 1526 and 1510 cm^{-1} . The band
8 assignments are listed in **Table 2** together with the bands found in amide I region. These
9 bands were assigned and discussed previously for pork muscle fiber tissue (21).

10 PLSR was performed to study the effect of the design factors on the FTIR spectra of
11 processed samples in the amide II region for the inside and skinside parts separately. The
12 respective correlation loading plots are shown in **Figures 5a** and **5b**. For the inside part (**5a**)
13 the first PLS component has an explained variance of 23% and 56% for **X** and **Y**,
14 respectively, whereas the second PLS component has an explained variance of 23% and 12%
15 in **X** and **Y**, respectively. For the skinside part (**5b**), the first PLS component has an explained
16 variance of 22% and 41% for **X** and **Y**, respectively, whereas the second PLS component has
17 an explained variance of 22% and 11% in **X** and **Y**. An interesting result is that the main
18 variation in the amide II region is due to smoking for both parts of fillet (inside and skinside).
19 Along PLS1, smoked samples are totally separated from non-smoked samples, whereas PLS2,
20 separated the samples with regards to salting time.

21 The amide II region is well known to be conformationally sensitive, although it is more
22 difficult to interpret than the amide I region. It is dominated by N-H bending (60%) and C-N
23 stretching (40%) vibrations. In addition, it has been suggested that the contribution of amino
24 acid side chains to the amide II region may be larger than in amide I region (37-39). As it has
25 been demonstrated in previous studies, the smoking process in some fish showed a decrease

1 in the availability of lysine (15-16). Riha and co-workers (15) revealed that carbonyl
2 compounds of liquid smoke solutions undergo a condensation reaction with amino groups of
3 proteins where lysine appeared to be the most reactive amino acid. Moreover, Sisko and co-
4 workers (16) also reported a lysine loss in smoked trout compared to non-smoked trout. We
5 may conclude that changes in amide II region could be related to interactions between smoke
6 components and amino groups from lysine or other N terminal of side chains more than
7 specific protein secondary structural changes. This is also confirmed by the fact that in this
8 kind of reactions N-H groups of proteins are interacting, which contribute strongly to the
9 amide II region.

10 **Comparison of light microscopy and FT-IR Microspectroscopy**

11 Both FTIR spectra and light microscopy images from salmon muscle tissue were compared
12 after introducing variation due to salting and smoking. A longer salting period resulted in
13 increased amounts of aggregated β structures and in decreased amounts of α -helical structures
14 as identified in the amide I region. These changes were related to observations made by light
15 microscopy where salted samples appeared to be more detached and their extracellular spaces
16 increased. However, smoking did not affect the same IR bands as salting. As it was observed
17 in amide I, the bands near 1639 cm^{-1} and 1609 cm^{-1} were decreased as a result of dehydration
18 and interactions between smoke components and amino acid side chains. Moreover, in the
19 amide II region, the major differences were caused by smoking. It is likely that the interaction
20 between carbonyl compounds of smoke and amino groups from lysine or other N terminal of
21 side chains is the main contributor to the FTIR signal in the amide II region. After smoking,
22 light images showed that the myofibers of the smoked samples appeared to be more shrunken
23 and their shape appeared more irregular and edged than for the non-smoked samples.
24 In conclusion, an understanding of the structural and chemical changes of food muscle
25 proteins in smoking processes is crucial for the production of high quality smoked products.

1 Most of the major quality issues in smoked salmon, such as water holding capacity and
2 texture, are related to myofibrillar proteins. In the present study it has been demonstrated for
3 the first time that FTIR microspectroscopy can be used to identify the interactions between
4 proteins and smoke components. Furthermore, it has been shown that salting time is an
5 important parameter in the cold smoking process, affecting the secondary structure of fish
6 proteins. Data from this study can provide an insight into the possibilities of FT-IR
7 microspectroscopy as a non-destructive technique to monitor processing-induced changes in
8 muscle tissues.

9 **Acknowledgements**

10 This study was supported by TRUEFOOD (Traditional United Europe Food), an Integrated
11 Project financed by the European Commission under the Sixth Framework Programme
12 (Contract n° FOOD-CT-2006-016264). The information in this document reflects only the
13 authors' views and the Community is not liable for any use that may be made of the
14 information contained therein. In addition funding by the Ministerio de Educación y Ciencia
15 (MEC, AGL-2006-01381) is gratefully acknowledged. I. Carton thanks Karin Solgaard, Frank
16 Lundby and Tom C. Johannessen for technical assistance and the Ministerio de Educación y
17 Ciencia for a Predoctoral Fellowship.

18

19 **LITERATURE CITED**

- 20 (1) Birkeland, S.; Rora, A. M. B.; Skara, T.; Bjerkeng, B. Effects of cold smoking
21 procedures and raw material characteristics on product yield and quality parameters of
22 cold smoked Atlantic salmon (*Salmo salar* L.) fillets. *Food Res. Int.* **2004**, 37, 273-286.
- 23 (2) Official Codex Standards. Recommended International code of practice for smoked fish.
24 CAC/RCP 25-1979, 9, 1-44.

- 1 (3) Hamm, R. *Functional properties of the myofibrillar system and their measurements. In:*
2 *Muscle as food*, ed.; Bechtel, P.J., Inc.: Academic Press, New York 1986, pp 135-199.
- 3 (4) Barat, J. M.; Rodriguez-Barona, S.; Andres, A.; Fito, P. Influence of increasing brine
4 concentration in the cod-salting process. *J. Food Sci.* **2002**, 67, 1922-1925.
- 5 (5) Böcker, U.; Kohler, A.; Aursand, I.G.; Ofstad, R. Effects of brine salting with regard to
6 raw material variation of Atlantic salmon (*Salmon salar*) muscle investigated by FT-IR
7 microspectroscopy *J. Agric. Food Chem.* **2008**, 56, 5129-5137.
- 8 (6) Suñen, E.; Fernandez-Galian, B.; Aristimuno, C. Antibacterial activity of smoke wood
9 condensates against *Aeromonas hydrophila*, *Yersinia enterocolitica* and *Listeria*
10 *monocytogenes* at low temperature. *Food Microbiol.* **2001**, 18, 387-393.
- 11 (7) Guillen, M. D.; Cabo, N. Study of the effects of smoke flavorings on the oxidative
12 stability of the lipids of pork adipose tissue by means of Fourier transform infrared
13 spectroscopy. *Meat Sci.* **2003**, 66, 647-657.
- 14 (8) Leroi, F.; Joffraud, J. J. Salt and smoke simultaneously affect chemical and sensory
15 quality of cold-smoked salmon during 5°C storage predicted using factorial design. *J.*
16 *Food Prot.* **2000**, 63, 1222-1227.
- 17 (9) Rorvik, L. M. *Listeria monocytogenes* in the smoked salmon industry. *Int. J. Food*
18 *Microbiol.* **2000**, 62, 183-190.
- 19 (10) Sigurgisladottir, S.; Sigurdardottir, M. S.; Ingvarsdottir, H.; Torrissen, O. J.;
20 Hafsteinsson, H. Microstructure and texture of fresh and smoked Atlantic salmon,
21 *Salmo salar* L., fillets from fish reared and slaughtered under different conditions.
22 *Aquac. Res.* **2001**, 32, 1-10.
- 23 (11) Hultmann, L.; Bencze Rora, A. M.; Steinsland, I.; Skara, T.; Rustad, T. Proteolytic
24 activity and properties of proteins in smoked salmon (*Salmo salar*) effects of smoking
25 temperature. *Food Chem.* **2003**, 85, 377-387.

- 1 (12) Gomez-Guillen, M. C.; Montero, P.; Hurtado, O.; Borderias, A. J. Biological
2 characteristics affect the quality of farmed Atlantic salmon and smoked muscle. *J. Food*
3 *Sci.* **2000**, 65, 53-60.
- 4 (13) Dvorak, Z.; Vognarova, I. Available lysine in meat and meat products. *J. Sci. Food*
5 *Agric.* **1965**, 16, 305-312.
- 6 (14) Chen, L.-B.; Issenberg, P. Interactions of some wood smoke components with e-amino
7 groups in proteins. *J. Agric. Food Chem.* **1972**, 20, 1113-1115.
- 8 (15) Riha, W. E.; Wendorff, W. L. Browning potential of liquid smoke solutions: comparison
9 of two methods. *J. Food Sci.* **1993**, 58, 671-674.
- 10 (16) Siskos, I.; Zotos, A.; Taylor, K. D. A. The effect of drying, pressure and processing time
11 on the quality of liquid-smoked trout (*Salmo gairdnerii*) fillets. *J. Sci. Food Agric.* **2005**,
12 85, 2054-2060.
- 13 (17) Metz B.; Kersten G.F.A.; Hoogerhout P.; Brugghe H.F; Timmermans H.A M; de Jong
14 A.; Meiring H.; Ten H.J.; Hennink W.E.; Crommelin D.J.A.; Jiskoot W. Identification
15 of formaldehyde-induced modifications in proteins: reactions with model peptides. *J.*
16 *Biol. Chem.* **2004**, 279, 6235-6243.
- 17 (18) Jackson, M.; Mantsch, H. H. The use and misuse of FTIR spectroscopy in the
18 determination of protein structure. *Crit. Rev. Biochem. Mol. Biol.* **1995**, 30, 95-120.
- 19 (19) Kirschner, C.; Ofstad, R.; Skarpeid, H. J.; Host, V.; Kohler, A. Monitoring of
20 denaturation processes in aged beef loin by Fourier transform infrared
21 microspectroscopy. *J. Agric. Food Chem.* **2004**, 52, 3920-3929.
- 22 (20) Böcker, U.; Ofstad, R.; Bertram, H. C.; Egelandsdal, B.; Kohler, A. Salt-induced
23 changes in pork myofibrillar tissue investigated by FT-IR microspectroscopy and light
24 microscopy. *J. Agric. Food Chem.* **2006**, 54, 6733-6740.

- 1 (21) Böcker, U.; Ofstad, R.; Wu, Z.; Bertram, H. C.; Sockalingum, G. D.; Manfait, M.;
2 Egelandsdal, B.; Kohler, A. Revealing covariance structures in Fourier transform
3 infrared and Raman microspectroscopy spectra: a study on pork muscle fiber tissue
4 subjected to different processing parameters. *Appl. Spectrosc.* **2007**, 61, 1032-1039.
- 5 (22) Wu, Z.; Bertram, H. C.; Kohler, A.; Böcker, U.; Ofstad, R.; Andersen, H. J. Influence of
6 Aging and salting on protein secondary structures and water distribution in uncooked
7 and cooked pork. A combined FT-IR microspectroscopy and ¹H NMR relaxometry
8 study. *J. Agric. Food Chem.* **2006**, 54, 8589-8597.
- 9 (23) Wu, Z.; Bertram, H. C.; Böcker, U.; Ofstad, R.; Kohler, A., Myowater dynamics and
10 protein secondary structural changes as affected by heating rate in three pork qualities: a
11 combined FT-IR microspectroscopic and ¹H NMR relaxometry study. *J. Agric. Food*
12 *Chem.* **2007**, 55, 3990-3997.
- 13 (24) Bertram, H. C.; Kohler, A.; Böcker, U.; Ofstad, R.; Andersen, H. J. Heat-induced
14 changes in myofibrillar protein structures and myowater of two pork qualities. A
15 combined FT-IR spectroscopy and low-field NMR relaxometry study. *J. Agric. Food*
16 *Chem.* **2006**, 54, 1740-1746.
- 17 (25) Engdahl, A.; Kolar, K., Metodeforskrift 22.6.93 Koksaltbestämning med Corning 926
18 Chloride Analyzer, Köttforskningsinstitut I Kävlinge, **1993**.
- 19 (26) Savitzky, A.; Golay, M.J.E., Smoothing and differentiation of data by simplified least
20 squares procedures. *Anal. Chem.* **1964**, 36, 1627-1639.
- 21 (27) Kohler, A.; Kirschner, C.; Oust, A.; Martens, H. Extended multiplicative signal
22 correction as a tool for separation and characterization of physical and chemical
23 information in Fourier transform infrared microscopy images of cryo-sections of beef
24 loin. *Appl. Spectrosc.* **2005**, 59, 707-716.

- 1 (28) Martens, H.; Martens, M., *Multivariate Analysis of Quality: An introduction*; ed.; John
2 Wiley & Sons Ltd: Chichester, UK, 2001.
- 3 (29) Aursand, I. G.; Veliyulin, E.; Böcker, U; Ofstad, R.; Rustad, T.; Erikson, U. Water and
4 salt distribution in Atlantic salmon (*Salmo salar*) studied by low-field ^1H -NMR, ^1H and
5 ^{23}Na MRI and light microscopy: Effects of raw material quality and brine salting. *J.*
6 *Agric Food.Chem.* **2009**, *57*, 46-54.
- 7 (30) Wang, D.; Tang, J.; Correia, L. R. Salt diffusivities and salt diffusion in farmed Atlantic
8 salmon muscle as influenced by rigor mortis. *J. Food Eng.* **2000**, *43*, 115-123.
- 9 (31) Segtnan, V.H.; Høy, M.; Sørheim, O.; Kohler, A.; Lundby, F.; Wold J. P.; Ofstad, R.
10 Non-contact salt and fat distributional analysis in salted and smoked salmon fillets using
11 X-ray computed tomography and NIR interactance imaging. *J. Agric. Food Chem.* **2008**,
12 (submitted).
- 13 (32) Cardinal, M.; Knockaert, C.; Torrissen, O.; Sigurgisladottir, S.; Morkore, T.;
14 Thomassen, M.; Vallet, J. L. Relation of smoking parameters to the yield, color and
15 sensory quality of smoked Atlantic salmon (*Salmo salar*). *Food Res. Int.* **2001**, *34*, 537-
16 550.
- 17 (33) Krimm, S.; Bandekar, J., Vibrational spectroscopy and conformation of peptides,
18 polypeptides, and proteins. *Adv. Prot. Chem.* **1986**, *38*, 181-364.
- 19 (34) Stafford, W. F. Effect of various anions on the stability of the coiled coil of skeletal
20 muscle myosin. *Biochem.* **1985**, *24*, 3314-3321.
- 21 (35) Jackson, M.; Choo, L. P.; Watson, P. H.; Halliday, W. C.; Mantsch, H. H. Beware of
22 connective-tissue proteins: Assignment and implications of collagen absorptions in
23 infrared-spectra of human tissues. *Biochim. Biophys. Acta* **1995**, *1270*, 1-6.

- 1 (36) Fabian, H; Mäntele, W. Infrared Spectroscopy of proteins. In: *Handbook of Vibrational*
2 *Spectroscopy*; Chalmers, J. M., Griffiths, P. R., Eds.; John Wiley & Sons Ltd.:
3 Chichester, U. K., 2002; pp 3399-3425.
- 4 (37) Chirgadze, Y. N.; Fedorov, O. V.; Trushina, N. P. Estimation of amino acid residue
5 side-chain absorption in the infrared spectra of protein solutions in heavy water.
6 *Biopolymers* **1975**, 14, 679-694.
- 7 (38) Venyaminov, S. Y.; Kalnin, N. N. Quantitative IR spectrophotometry of peptide
8 compounds in water (H₂O) solutions. I. Spectral parameters of amino acid residue
9 absorption bands. *Biopolymers* **1990**, 30, 1243-1257.
- 10 (39) Fabian, H.; Naumann, D. Methods to study protein folding by stopped-flow FT-IR.
11 *Methods* **2004**, 34, 28-40.

12

Table 1. General sample characteristics for non-smoked and smoked salmon fillets. H indicates samples from head and T samples from the tail region of the fillet.

Size (Location)	% Weight Loss		% NaCl ^(s)		% fat		
	24 hours	8 hours	24 hours	8 hours	24 hours	8 hours	
Non-smoked	small (H)	6,36	5,50	2,47±0,07	1,57±0,03**	18,9±0,4	14,4±0,1
				(T)	3,88±0,16 ^c	2,29±0,06** ^c	4,3±0,2
	medium (H)	6,24	4,85	2,46±0,07	1,63±0,03**	16,2±0,4	17,9±0,1
				(T)	3,28±0,12 ^b	1,79±0,04** ^b	7,0±0,4
	large (H)	6,74	4,23	1,91±0,04	1,76±0,03*	17,8±0,1	18,1±0,1
				(T)	3,32±0,12 ^c	2,29±0,06** ^c	8,3±0,0
Smoked	small (H)	9,77	9,17	3,57±0,07 ^C	2,05±0,07** ^C	15,6±0,5	16,7 ±0,0
				(T)	4,74±0,22 ^{b,B}	2,87±0,09** ^{c,B}	5,4±0,1
	medium (H)	8,91	7,41	2,47±0,07 ^A	1,52±0,07** ^B	19,6±0,4	16,1±0,5
				(T)	2,54±0,08 ^{a,C}	2,46±0,07 ^{ns,c,C}	5,8±0,0
	large (H)	8,86	7,51	3,17±0,07 ^C	1,95±0,07** ^B	19,8±0,2	14,3±0,5
				(T)	4,08±0,18 ^{b,B}	2,50±0,07** ^{c,A}	7,0±0,4

(s) Significance level. Between salted for 24 h and 8 h: ns, not significant; * p < 0.05; ** p < 0.01. Between head and tail samples: a, not significant; b, p < 0.05; c, p < 0.01. Between non-smoked and smoked samples: A, not significant; B, p < 0.05; C, p < 0.01.

Table 2. IR region, FT-IR frequencies and approximate descriptions of vibrational modes.

Region	Frequency (cm⁻¹)	Tentative band assignment
<i>Amide I</i>	1694	Aggregated β -sheet structures (intramolecular)
	1682	Antiparallel β -sheet structures (intramolecular)
	1667	Non- hydrogenated C=O groups
	1658	Loop structures
	1653	α -helical structures
	1639	Antiparallel β -sheet structures / O-H bending of water
	1628	Aggregated β -sheet structures (intramolecular)
	1619	Aggregated β -sheet structures (intermolecular)
	1609	Amino acid side chains (tentatively)
<i>Amide II</i>	1584	α -helical structures
	1574	Unspecified
	1567	Residue and/ or possibly aggregated β -sheet structures
	1555	Unspecified
	1544	α -helical structures
	1534	Denatured random structures
	1526	Aggregated β -sheet structures (tentatively)
	1510	Tyrosine (tentatively)

FIGURE CAPTIONS

Figure 1. Transverse sections of salmon muscle stained with Toluidine Blue. **S** refers to skin side and **I** to inside, **U** to unprocessed samples, **S8** refers to salted for 8 hours, **S24** salted for 24 hours, **B8** salted for 8 hours followed by smoking and **B24** salted for 24 hours followed by smoking . All images shown were derived from the head region of the salmon.

Figure 2. Typical FTIR spectrum of a single myofiber obtained from unprocessed salmon muscle cryosection showing the spectral range from 4000-1000 cm^{-1} . (Inset) Positive second-derivative spectra of the same unprocessed sample together with a processed sample in the amide I region.

Figure 3. PCA score plot of non-averaged samples (144 samples) using the selected wavenumbers of the inverted 2nd derivative in the amide I region as variables. Marked in red: salted; in blue smoked; S and I represent skinside and inside samples, respectively. The explained variance by PC1 and PC2 is 46% and 34%, respectively.

Figure 4a/b. Correlation loading plots of PLSR with design parameters as **X** and selected wavenumbers of the inverted 2nd derivative in the amide I region as **Y**. The inner and outer circles in the figure refer to 50 and 100% explained variance, respectively. For the inside part samples (**4a**) the explained variance in **X** and **Y** for PLS component 1 and 2 are 23%, 23 % for **X** and 36% and 21% for **Y**. For the skinside part samples (**4b**) the explained variance in **X** and **Y** for PLS component 1 and 2 are 22% and 22% (for **X**) and 32% and 14% (for **Y**), respectively.

Figure 5a/b. Correlation loading plots of PLSR with design parameters as **X** and selected wavenumbers in the amide II region of the negative 2nd derivative spectra as **Y**. The inner and outer circles in the figure refer to 50 and 100% explained variance, respectively. For the inside part (**5a**) the first PLS component has an explained variance of 23% and 56% for **X** and **Y**, respectively, whereas the second PLS component has an explained variance of 23% and

12% in **X** and **Y**. For the skinside part (**5b**), the first PLS component has an explained variance of 22% and 41% for **X** and **Y**, respectively, whereas the second PLS component has an explained variance of 22% and 11% in **X** and **Y**.

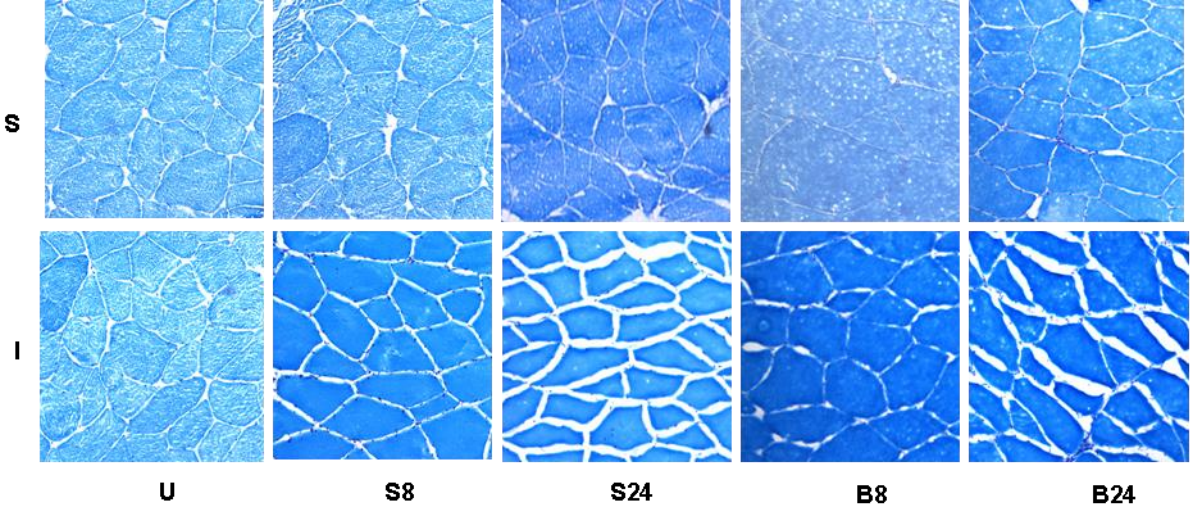


Figure 1

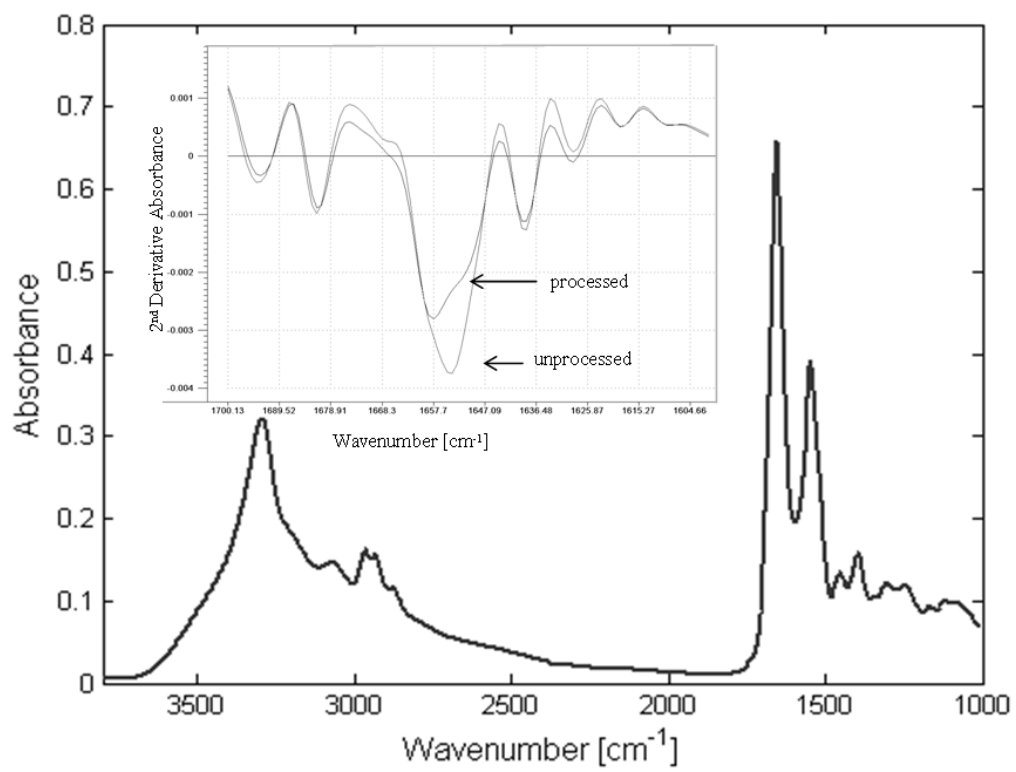


Figure 2

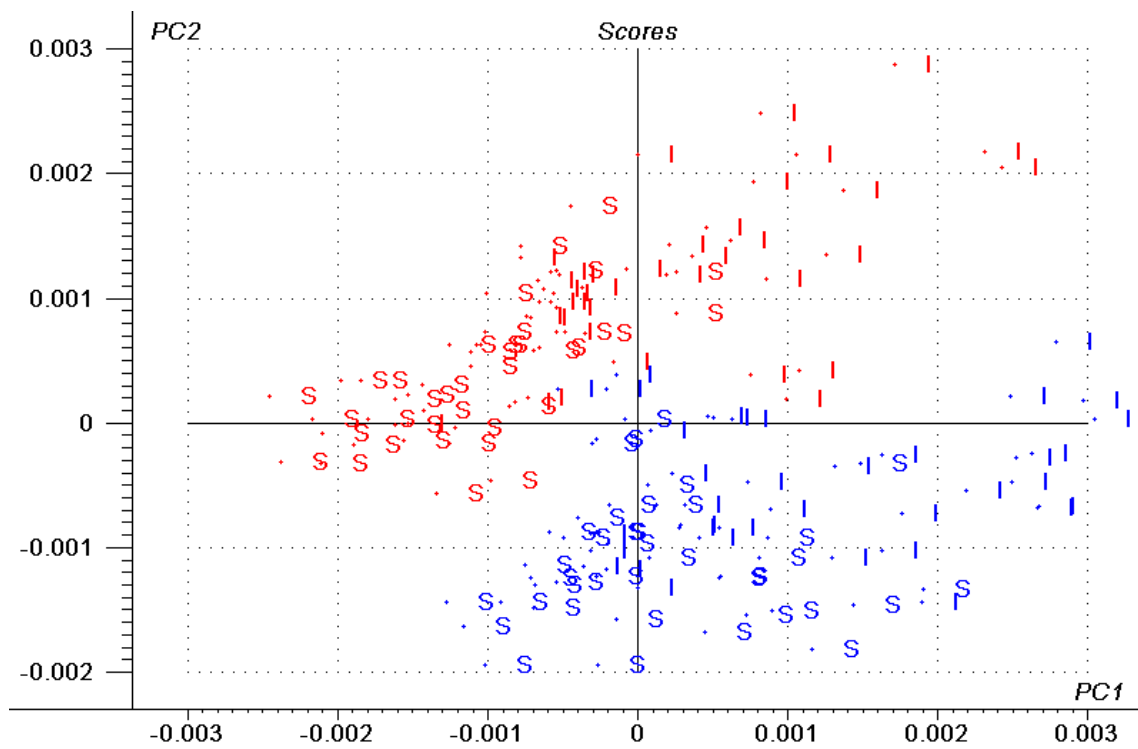


Figure 3

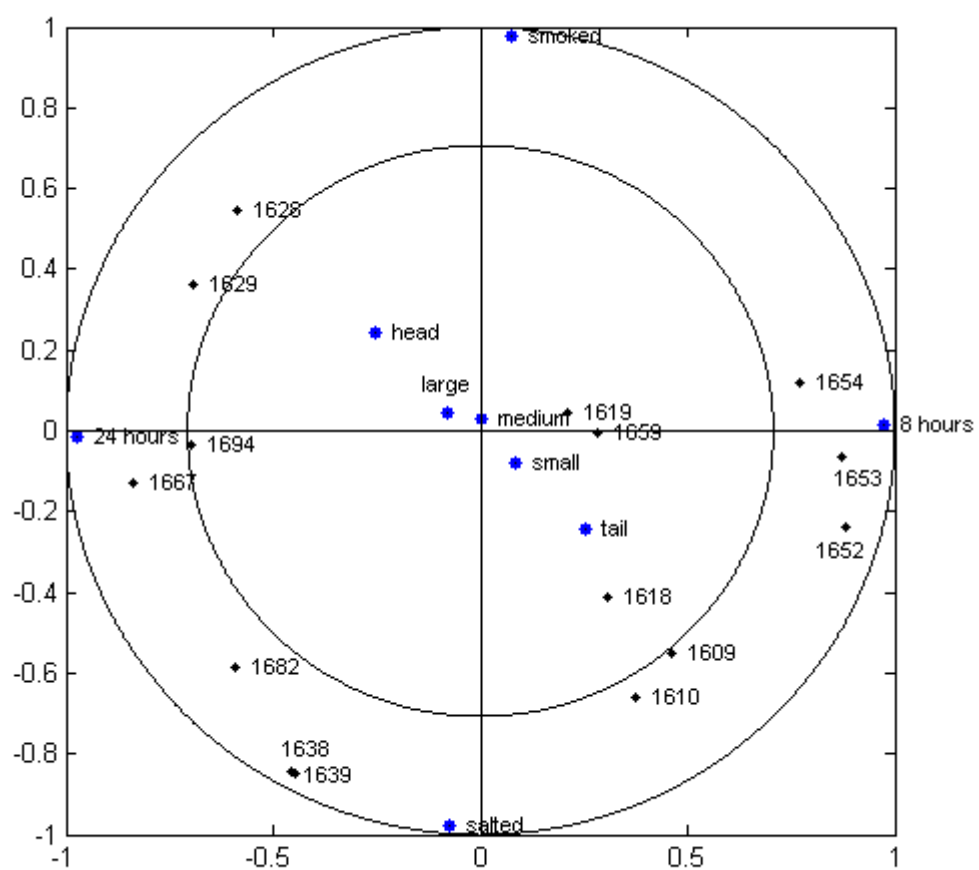


Figure 4a

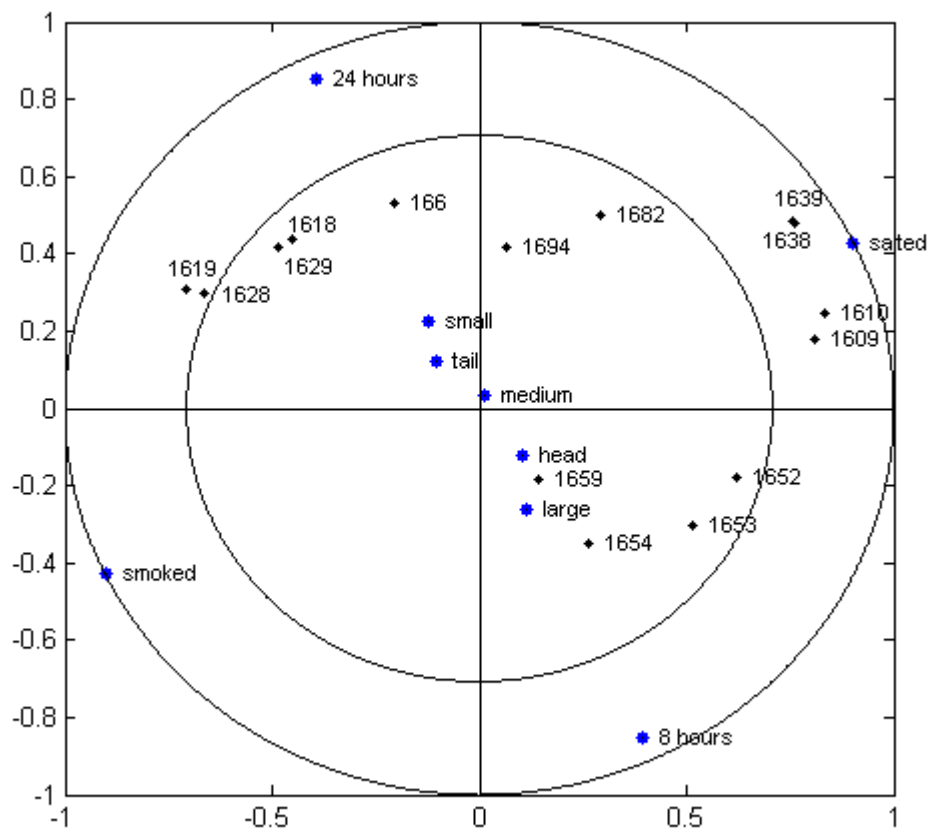


Figure 4b

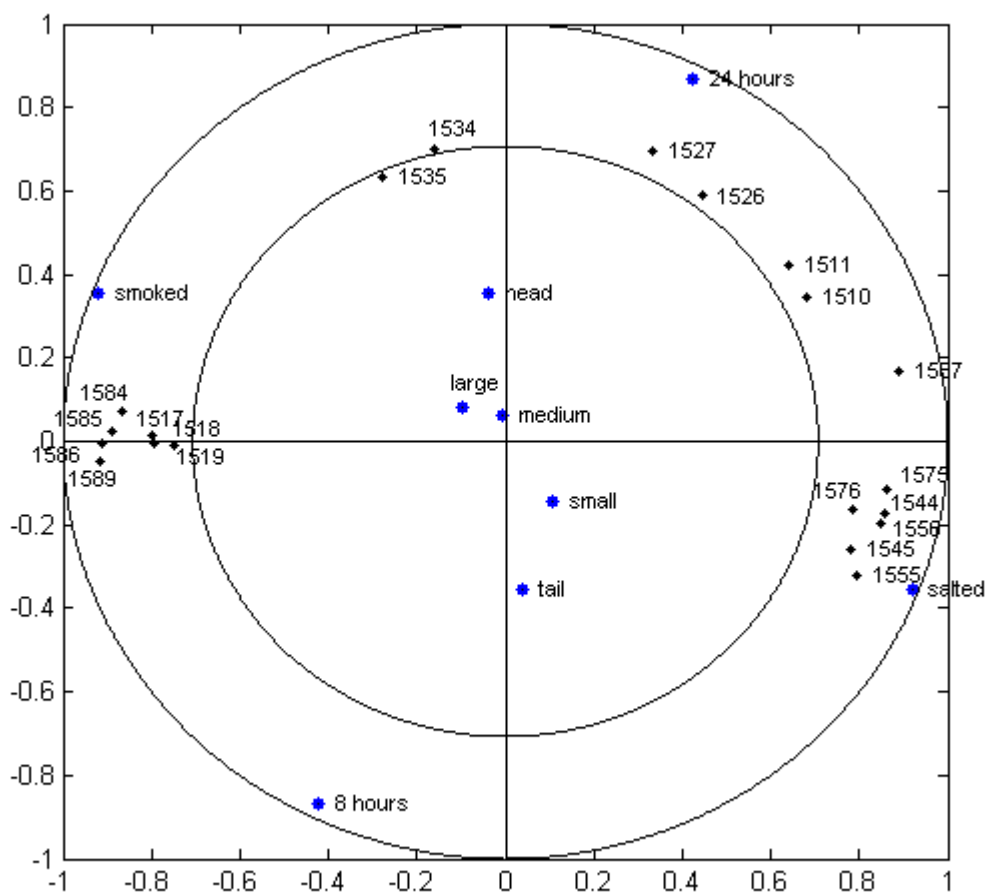


Figure 5a

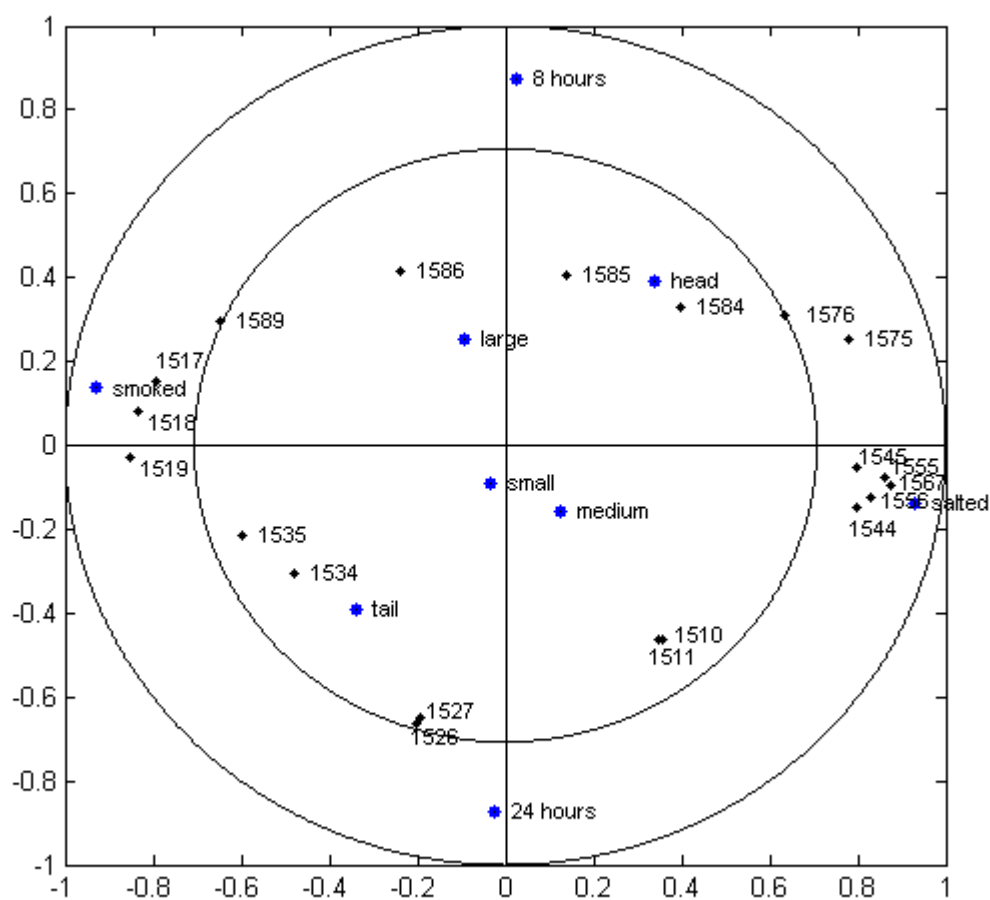


Figure 5b